ISSN:3007-9640 DOI: https://doi.org/10.70114/acmsr.2025.2.1.P383

Real-Time Optimization Method for Virtual Inertia Based on Energy Storage VSG Grid-Connected Control

Guangjie Li [a] *, Jing Bu [b], Biao Yue

Nanjing University of Science and Technology, Nanjing, China;

[a] 1135167898@qq.com, [b] bujing30@foxmail.com

Abstract. Grid-forming energy storage controlled in Virtual Synchronous Generator (VSG) has received widespread attention due to its ability to improve system inertia level and to support renewable energy's friendly grid-connection. However, when using VSG control with fixed virtual inertia to deal with different frequency events, its virtual rotational speed and power angle are prone to significant oscillating and slow recovery. Therefore, this article proposes a method for dynamically optimizing virtual inertia in real-time based on status of virtual speed and power angle. Firstly, a mathematical model of energy storage based on VSG control was constructed, and the influence of virtual inertia on the transient processes of virtual speed and power angle was analyzed. Secondly, the optimization objective is to reduce virtual speed oscillation, power angle oscillation, and shorten transition time. The range of virtual inertia values is determined with system stability as the constraint. Then the optimization model is established. The particle swarm optimization algorithm is used to calculate the optimal inertia value in real time. Finally, a simulation model of a wind storage joint system with VSG control was constructed, and the effectiveness of the proposed method was verified.

Keywords: virtual synchronous generator rotor inertia; fluctuations of frequency and power angle; particle swarm optimization algorithm; wind storage combined system.

1. Introduction

VSG control is one of the mainstream grid-forming control strategies. However, traditional VSG control employs fixed virtual inertia, failing to leverage the flexible controllability of converters. This results in poor dynamic performance of the virtual speed and power angle during transient processes when disturbances occur in the system[1], leading to issues such as large fluctuations and slow recovery. Therefore, literature[2] introduced the bang-bang control strategy, which allows inertia to switch between larger and smaller values, making it simple to set but with limited effectiveness. Meanwhile, literature[3-6] achieved adaptive adjustment of the virtual rotor inertia by constructing a functional relationship between the rotor inertia and both the speed deviation and the rate of speed change. However, this method focuses only on the recovery of the VSG speed and does not consider the dynamic process of the VSG power angle. Additionally, they did not delve into specific methods for determining the initial inertia and adjustment coefficients. Thus, literature[7,8] used optimization algorithms to obtain the initial inertia and adjustment coefficients in the function construction method, but the optimization was done offline, lacking real-time responsiveness. Literature[9,10] adopted fuzzy control strategies to determine the value of virtual inertia, essentially similar to the function construction method;

To address this problem, this paper simultaneously considers the dynamic performance of both virtual speed and power angle, proposing a real-time optimization method to adjust the virtual inertia of the VSG. This paper constructs an optimization model and the optimal value of virtual inertia is obtained by solving it online. The results demonstrate that the proposed method plays a crucial role in enhancing the control performance of the VSG.

ISSN:3007-9640 DOI: https://doi.org/10.70114/acmsr.2025.2.1.P383

2. Grid-connection Analysis of Energy Storage VSG

2.1 VSG Control Principle

Grid-forming energy storage using VSG control is typically integrated with new renewable energy generation to provide inertia support to the system. When there are significant variations in the output of new energy sources, the virtual speed and power angle of the VSG-based energy storage fluctuate dramatically.

The active-power-frequency control part of VSG control simulates the rotor motion equation of synchronous generators to control the active power output. According to its typical active power control and system structure, the following can be expressed:

$$\begin{cases} \dfrac{P_{\text{ref}} - P_{\text{e}}}{\omega_0} - D\Delta\omega = J\dfrac{\mathrm{d}\Delta\omega}{\mathrm{d}t} \\ \Delta\omega = \omega - \omega_0 \\ P_{\text{e}} = P_{\text{L}} + P_{\text{g}} \end{cases} \tag{1}$$

Where, P_{ref} is the given active power, P_{e} is the actual output active power,ω_0 is the rated speed, $\omega_0=2\pi f_0=100\pi$ rad/s, J is the virtual inertia, D is the damping coefficient, θ is the voltage phase angle, P_{g} is the power transmitted from the energy storage VSG to the grid, P_{L} is the power provided by the energy storage VSG to the local load, ω is the current speed of the VSG, $\Delta\omega$ is the deviation of the VSG speed.

Assuming that the voltage and frequency of the grid remain almost unchanged, and since the power angle δ is usually small, the power-angle characteristic equation of the VSG can be expressed as:

$$\frac{\mathrm{d}\delta}{\mathrm{d}t} = \Delta\omega \tag{2}$$

$$P_{\text{g}} = \frac{U_{\text{s}} E_{\text{g}}}{X_{\text{g}}}\delta = \text{K}\delta \tag{3}$$

Where, U_{s}、 E_{g} represent the bus voltage at the VSG outlet and the grid voltage; δ is the power angle； The value of K varies depending on different systems and can be calculated based on measurements of P_{g} and δ under various steady-state conditions.

2.2 Impact of *J* on Power Angle

By linearizing equations (1), (2), and (3) and applying the Laplace transform, the closed-loop transfer function for active power control can be derived as:

$$G(s) = \frac{P_{\text{g}}(s)}{P_{\text{ref}}(s) - P_{\text{L}}(s)} = \frac{\text{K}}{J\omega_0} \cdot \frac{1}{s^2 + \dfrac{D}{J}s + \dfrac{\text{K}}{J\omega_0}} \tag{4}$$

By comparing with the transfer function of the second-order canonical system, the natural frequency ω_{n} and damping ratio ζ can be derived. Subsequently, the overshoot and settling time of the second-order system can be calculated. The results indicate that both the overshoot and settling time of the power angle curve increase with the growth of *J*. These outcomes are demonstrated in the power angle curve illustrated in Figure 1 below.

ISSN:3007-9640 DOI: https://doi.org/10.70114/acmsr.2025.2.1.P383

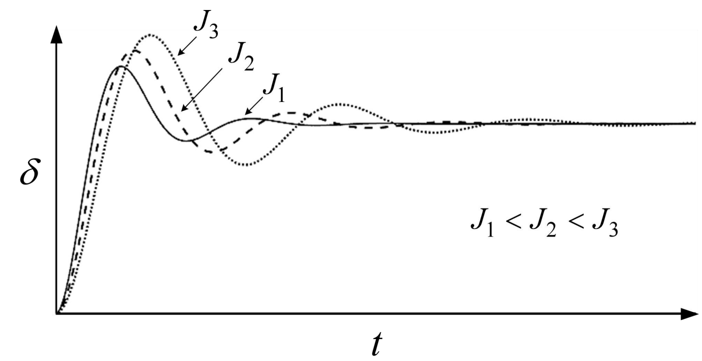

Fig. 1 Comparison of power angle curves of VSG under different J values

2.3 Impact of J on Virtual Speed

According to equations (1), (2), and (3), if the system is in steady-state at t=t_0, i.e., ω=ω_0, P_{ref}-P_{e}=0, then for t>t_0, the grid connection of the VSG satisfies the following equation:

$$-\mathrm{K}\int_{t_0}^{t}\Delta\omega \mathrm{d}t-\Delta P_{\mathrm{L}}-D\omega_0\Delta\omega=J\omega_0\frac{\mathrm{d}\Delta\omega}{\mathrm{d}t} \tag{5}$$

Where, ΔP_{L} represents the system's unbalanced power, caused by events such as load switching and wind speed fluctuations. When the system's $\Delta\omega$ and d$\Delta\omega$/dt are known, substituting these values into equation (5) will yield the unbalanced power at that moment.

Let t>0>t_0. Solving this second-order linear nonhomogeneous differential equation yields the power angle curve y for t>0:

$$y=e^{-\frac{D}{2J}t}(C_1\cos\beta t+C_2\sin\beta t)-\frac{\Delta P_{\mathrm{L}}}{\mathrm{K}} \tag{6}$$

Where, $\beta=\frac{\sqrt{4J\omega_0\mathrm{K}-D^2\omega_0{}^2}}{2J\omega_0}$; C_1 and C_2 are determined by the initial state of the system at t=0.

Taking the derivative of y yields the expression for the speed variation curve:

$$y'=\Delta\omega(t)=e^{-\frac{D}{2J}t}(\Delta\omega_{on}\cos\beta t-d\sin\beta t) \tag{7}$$

Where, $d=\frac{D\omega_0\Delta\omega_{\mathrm{on}}+2\Delta P_{\mathrm{L}}}{\sqrt{4J\omega_0\mathrm{K}-D^2\omega_0{}^2}}$; $\Delta\omega_{\text{on}}$ is determined by the initial state of the system at t=0.

From the expression, the speed deviation curve is an oscillatory decay, with the decay rate dependent on the exponential term $D/2J$. Therefore, the recovery time of the speed increases as the inertia J increases. Additionally, calculations show that the overshoot of the rotational speed is negatively correlated with the inertia. Given the relationship between speed and frequency ω=2πf, the results are reflected in the VSG output frequency curve as shown in Figure 2.

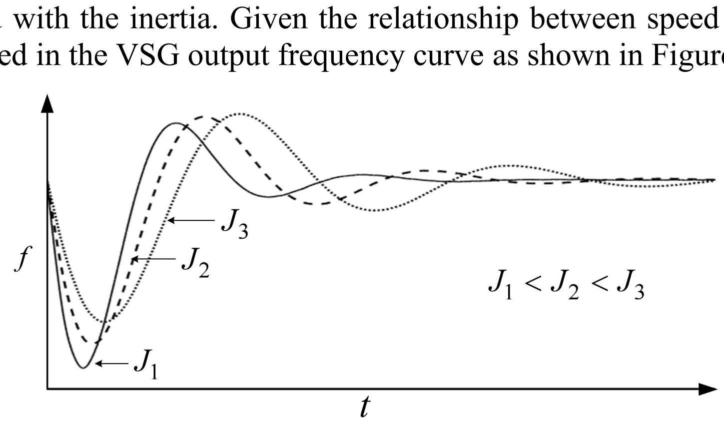

Fig. 2 Comparison of VSG output frequency curves under different J values

ISSN:3007-9640 DOI: https://doi.org/10.70114/acmsr.2025.2.1.P383

3. Real-time Optimization Method for Virtual Inertia

3.1 Object Function

To comprehensively consider the dynamic performance of frequency and power angle, this paper constructs the objective function based on the aforementioned mathematical derivation as follows:

$$\min F = Q^2 \cdot \Delta\omega_{\max}{}^2 + R^2 \cdot \int_0^{t_p} \Delta\delta^2 \mathrm{d}t + T^2 \cdot t_p{}^2 \tag{8}$$

Where, F is the fitness function; $\Delta\omega_{max}$ is the maximum speed deviation; $\int\Delta\delta^2 \mathrm{d}t$ is the integral of the squared power angle change, used to characterize the degree of power angle fluctuation; t_p is the time required for the speed to recover to the vicinity of ω_0. Q, R, and T are weight coefficients, set according to the actual operating conditions of the system.

3.2 Constraint Conditions

In order to meet the minimum inertia level requirements of the system and ensure system stability—specifically, ensuring that the damping ratio satisfies $\zeta \in (0,1)$ to avoid oscillatory divergence, the lower limit of inertia J_{min} can be determined.

Additionally, in practical applications, the upper limit of inertia J_{max} should be determined based on actual operating conditions and performance requirements[4], such as:

$$J \le \frac{\Delta P_{\max}}{\max\left\{\Delta\omega \cdot (\mathrm{d}\Delta\omega / \mathrm{d}t)\right\}} \tag{9}$$

In this equation, ΔP_{max} represents the maximum deviation of the VSG output power relative to the rated power.

Through the above analysis of system requirements, J must satisfy:

$$J_{\min} < J < J_{\max} \tag{10}$$

3.3 Optimization Methods

This paper employs the Particle Swarm Optimization algorithm to solve the objective function. The algorithm is initiated by setting thresholds for the speed deviation and the rate of speed change. The initial value of the inertia is set to J_0, and this value is output when the algorithm is not activated. Consequently, the complete control block diagram for the active power control of the VSG is obtained, as shown in Figure 3 below.

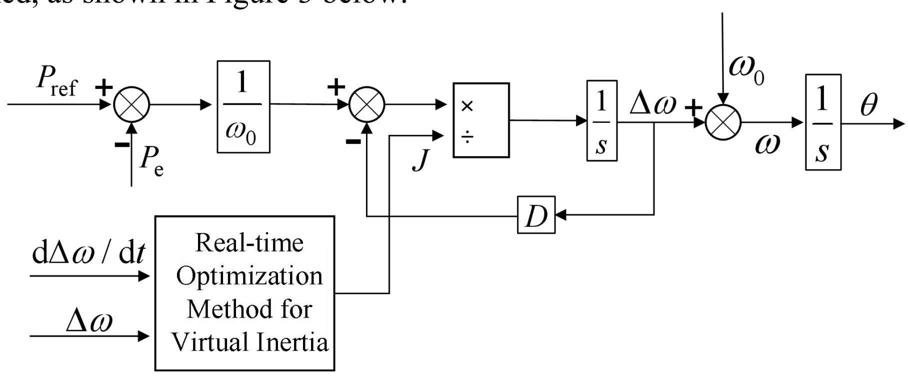

Fig. 3 Complete control diagram of VSG active power control

ISSN:3007-9640 DOI: https://doi.org/10.70114/acmsr.2025.2.1.P383

4. Simulation Analysis

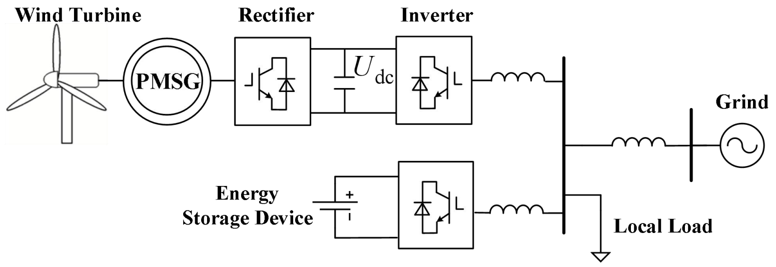

Fig. 4 Simulation System Diagram

To validate the proposed method, this paper builds a simulation model of a wind-storage hybrid system with VSG control on the Matlab/Simulink platform, as shown in Figure 4. The system parameters are listed in Table 1.

Table 1. Simulation parameter table

Parameter	Value
Bus Voltage	690 V
Grid Frequency	50 Hz
Energy Storage Rated Power	400 kW
Wind Turbine Capacity	600 kW
DC Voltage	1800 V
VSG Initial Inertia J0	12 kg·m²

To demonstrate the effectiveness of the proposed method, this paper compares it with the simulation results of a traditional inertia adaptation algorithm. The traditional inertia adaptation algorithm is described as follows:

$$J=\begin{cases} J_0 & \Delta\omega(\mathrm{d}\Delta\omega/\mathrm{d}t)\le 0 \\ J_0 & \left|\mathrm{d}\Delta\omega/\mathrm{d}t\right|\le T_j \\ J_0+k_j\left|\dfrac{\mathrm{d}\Delta\omega}{\mathrm{d}t}\right| & \Delta\omega(\mathrm{d}\Delta\omega/\mathrm{d}t)>0\cap\left|\mathrm{d}\Delta\omega/\mathrm{d}t\right|>T_j \end{cases} \tag{11}$$

Where, T_j is the threshold, and k_j is the adjustment coefficient.

In the initial experiment, the system is set to operate in a steady state. The range of inertia is set to [6, 45]. At 4.5 seconds, the input wind speed to the wind turbine is increased by 1m/s. The changes in the output voltage frequency and power angle of the wind-storage hybrid system under different methods are compared, as shown in Figures 5 and 6. The changes in inertia output by the algorithm are shown in Figure 7.

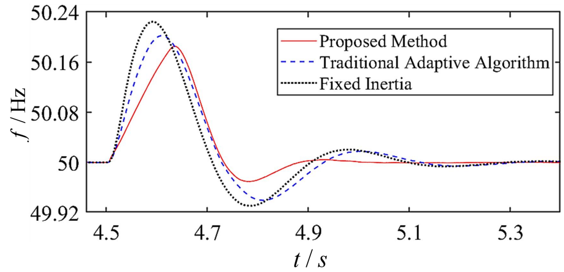

Fig. 5 Comparison chart of output frequency under different methods

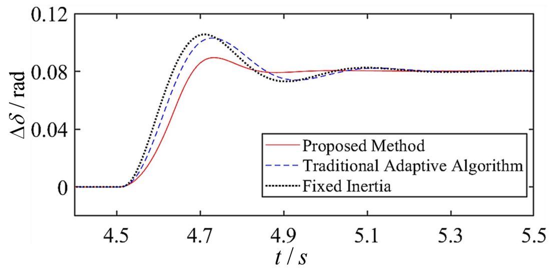

Fig. 6 Comparison chart of changes in power angle under different methods

ISSN:3007-9640 DOI: https://doi.org/10.70114/acmsr.2025.2.1.P383

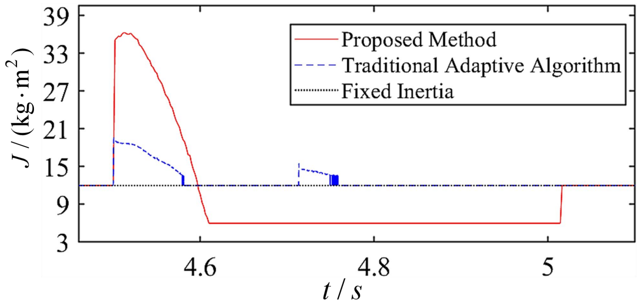

Fig. 7 VSG inertia variation curve

From Figures 5 and 6, it can be observed that when using the method proposed in this paper, the system output frequency and power angle exhibit the least fluctuations and return to steady state faster. Figure 7 shows that the traditional adaptive algorithm adjusts inertia near the peaks and troughs of the frequency curve to suppress frequency deviations; however, due to the initial frequency overshoot, the proposed real-time optimization method applies a larger inertia initially to suppress frequency deviations. As the frequency overshoot decreases significantly, the algorithm reduces inertia to accelerate frequency recovery. When the transient process is nearing completion, inertia returns to its initial value J_0. Since the inertia reaches the set lower limit, it remains constant thereafter.

Three indicators—frequency overshoot $|\Delta f|_{max}$, power angle overshoot $|\Delta \delta|_{max}$, and the time Δt required to recover to steady state—are used to compare the effectiveness of the three methods, as shown in Table 2.

Table 2. Comparison table of performance indicators when wind speed changes

Method	$\|\Delta f\|_{max}$	$\|\Delta \delta\|_{max}$	Δt
Proposed Method	0.169Hz	0.088rad	2.475s
Traditional Adaptive Algorithm	0.184Hz	0.100rad	2.690s
Fixed Inertia	0.204Hz	0.106rad	2.656s

From the data in the table, it can be seen that all three indicators are the smallest in the proposed method, indicating that the performance is the best.

5. Summary

To address the issues of significant fluctuations and slow recovery in virtual speed and power angle when using fixed virtual inertia in energy storage VSG, this paper proposes a real-time optimization method for virtual inertia. An optimization model is constructed by deriving the impact of inertia on VSG speed and power angle, and an optimization algorithm is employed to obtain the optimal inertia in real time. Simulation results demonstrate that the proposed method effectively enhances the dynamic performance of power angle and frequency regulation, significantly improving the flexibility of VSG control. Future research could further explore the weighting coefficients in the objective function.

Acknowledgements

Project Name: Coordinated Stability Support Technology for Large-Scale Renewable Energy Integration and Multi-Terminal DC Infeed in Receiving-End Grids;

Research Topic Title: “4.1 Coordinated Stability Support Technology for Large-Scale Renewable Energy Integration and Multi-Terminal DC Infeed in Receiving-End Grids(Common Key Technology Category)”;

Project Code: 2024YFB2408900.

ISSN:3007-9640 DOI: https://doi.org/10.70114/acmsr.2025.2.1.P383

References

[1] WANG Xiaodong, CAO Guosheng, LIU Yingming, et al. Re-search on dynamic virtual inertia and damping fuzzy adaptive control strategy for doubly fed wind turbines[J]. Acta Energiae Solaris Sinica, 2023, 44(9): 356-365.

[2] M. M. Elwakil, H. M. E. Zoghaby, S. M. Sharaf and M. A. Mosa. Adaptive virtual synchronous generator control using optimized bang-bang for Islanded microgrid stability improvement[J]. Protection and Control of Modern Power Systems, 2023, 8(4): 1-21.

[3] CHENG Chong, YANG Huan, ZENG Zheng, et al. Adaptive control method for rotor inertia of virtual synchronous generator[J]. Automation of Electric Power Systems, 2015(19): 82-89.

[4] YANG Yun, MEI Fei, ZHANG Chenyu, et al. Collaborative adaptive control strategy for rotational inertia and damping coefficient of virtual synchronous generator[J]. Electric Power Automation Equipment, 2019, 39(3): 125-131.

[5] M. Ren, T. Li, K. Shi, P. Xu and Y. Sun. Coordinated Control Strategy of Virtual Synchronous Generator Based on Adaptive Moment of Inertia and Virtual Impedance[J]. IEEE Journal on Emerging and Selected Topics in Circuits and Systems. 2021, 11(1): 99-110.

[6] X. Hou, Y. Sun, X. Zhang, J. Lu, P. Wang and J. M. Guerrero. Improvement of Frequency Regulation in VSG-Based AC Microgrid Via Adaptive Virtual Inertia[J]. IEEE Transactions on Power Electronics, 2020, 35(2): 1589-1602.

[7] GUO Jianyi, FAN Youping. Adaptive Control Strategy for VSG Parameters Based on Improved Particle Swarm Optimization Algorithm[J]. Electric Machines and Control, 2022, 26(6): 72-82.

[8] T. Shi., J. Sun, X. Han, C. Tang. Research on adaptive optimal control strategy of virtual synchronous generator inertia and damping parameters[J]. IET Power Electron, 2024, 17: 121-133.

[9] V. Thomas, K. S. and S. Ashok. Fuzzy Controller-Based Self-Adaptive Virtual Synchronous Machine for Microgrid Application[J]. IEEE Transactions on Energy Conversion, 2021, 36(3): 2427-2437.

[10] B. Long, Y. Liao, K. T. Chong, J. Rodríguez and J. M. Guerrero. Enhancement of Frequency Regulation in AC Microgrid: A Fuzzy-MPC Controlled Virtual Synchronous Generator[J]. IEEE Transactions on Smart Grid, 2021, 12(4): 3138-3149.